Biomed Microdevices (2009) 11:421–427
DOI 10.1007/s10544-008-9248-6

Elastic and viscoelastic characterization of microcapsules for drug delivery using a force-feedback MEMS microgripper

Keekyoung Kim · Xinyu Liu · Yong Zhang · Ji Cheng · Xiao Yu Wu · Yu Sun

Published online: 18 November 2008

Abstract This paper reports a monolithic, force-feedback MEMS (microelectomechanical systems) microgripper and its application to micro-scale compression testing of swollen hydrogel microcapsules at wet state during manipulation. The single-chip microgripper integrates an electrothermal microactuator and two capacitive force sensors, one for contact detection (force resolution: 38.5 nN) and the other for gripping force measurements (force resolution: 19.9 nN). With the capability of resolving gripping forces down to 19.9 nN and material deformations with a 20.5 nm resolution, the system quantified Young's modulus values and viscoelastic parameters of alginate microcapsules (15–25 μm), demonstrating an easy-to-operate, accurate compression testing technique for characterizing soft, micrometer-sized biomaterials.

Keywords MEMS microgripper · Micro-scale compression testing · Hydrogel microcapsule · Young's modulus · Viscoelastic parameters

K. Kim · X. Liu · Y. Zhang · Y. Sun (✉)
Advanced Micro and Nanosystems Laboratory,
University of Toronto, 5 King's College Road,
Toronto, Ontario M5S 3G8, Canada
e-mail: sun@mie.utoronto.ca

J. Cheng · X. Yu Wu
Leslie Dan Faculty of Pharmacy,
University of Toronto, 144 College Street,
Toronto, Ontario M5S 3M2, Canada

1 Introduction

Hydrogel microcapsules used for drug delivery or cell encapsulation are highly deformable with diameters from 1 μm to 100 μm, comparable to the size of most biological cells. The mechanical properties of microcapsules determine whether they can survive the stress in the needle tract during injection, in the blood capillaries, or in the applied tissues. Maintaining their integrity during processing and application is essential for preventing dose dumping, cell death and/or immunoresponse as well as for achieving desired performance. To mechanically characterize soft hydrogel microparticles, a system capable of accurately measuring low-magnitude forces and microscopic material deformations is required.

Different from local probing techniques such as optical tweezers (Fontes et al. 2008), micropipette aspiration (Hochmuth 2000), atomic force microscopy (AFM) (Dulinska et al. 2006), and magnetic bead measurement (Bausch et al. 1999), micro-scale compression testing permits the quantification of mechanical parameters globally. Micro-scale compression using a commercial force transducer with an assembled optical fiber probe was demonstrated for investigating the bursting forces of single tomato cells (Blewett et al. 2000). AFM tip with an assembled colloid sphere has also been reported as a micro-scale compression tool for determining Young's modulus of polyelectrolyte microcapsules (Lulevich and Vinogradova 2004).

In the pursuit of monolithic devices for mechanical characterization of biomaterials, many MEMS-based force sensors have been developed. MEMS piezoresistive force sensors were demonstrated for the measurement of contractile forces of individual heart cells

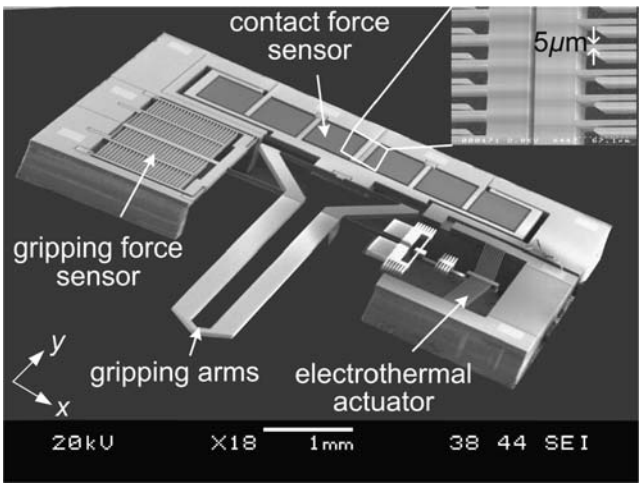

Fig. 1 MEMS microgripper with integrated two-axis force sensors

(Lin et al. 2001). Based on visual deformation measurements of flexible beams, MEMS force sensors were developed for studying cell mechanics (Yang and Saif 2005). MEMS capacitive force sensors were also developed for characterizing flight behavior of fruit flies (Sun et al. 2005) and mechanical properties of mouse oocytes and embryos (Sun et al. 2003).

Compared with force sensors, force-feedback MEMS microgrippers have the distinct capability of manipulating micrometer-sized biomaterials (e.g., pick-transport-place) and simultaneously quantifying their mechanical properties. Recently, MEMS microgrippers with a single-axis force sensor were demonstrated for open-loop micrograsping (Beyeler et al. 2007) and for investigating charge transport through DNA (Yamahata et al. 2008).

The MEMS microgripper (Fig. 1) developed in this work for the manipulation and characterization of hydrogel microcapsules integrates two-axis force feedback to protect the fragile microgripper by detecting contact between the microgripper and the substrate; and to provide gripping force feedback for achieving secured grasping without applying excessive gripping forces.

The microcapsules studied in this work were made from biodegradable and biocompatible hydrogel materials, alginate coated with chitosan, with applications to the delivery of drugs, enzymes, and living cells. The variation in the percentage of chitosan coating changes the mechanical properties of the microcapsules and can be utilized to achieve desired drug release rates/profiles. Enabled by the force-feedback MEMS microgripper, the mechanical properties of alginate microcapsules with 1%, 2%, and 3% chitoan coating at wet state were determined. This study produced useful data and guidelines for selecting materials and formulations of microcapsules.

2 Development of force-feedback MEMS microgrippers

Using an SOI (silicon on insulator) wafer, the MEMS microgrippers were fabricated through the process shown in Fig. 2. The process etches both handle (350 μm thick) and device (50 μm thick) Si layers, permits electrical isolation and mechanical connection, creates a step difference on suspended movable frames to enhance device robustness for handling, and enables dice free device release. Design and fabrication details of the microgripper have been reported in Kim et al. (2008).

Briefly, to achieve a high sensitivity and linear input-output relationship, transverse tri-plate differential comb drives shown in Fig. 3 are used (Sun et al. 2005). Capacitances are

$$C_{x1} = n\frac{K\varepsilon_0 tl}{d_{x1}} + n\frac{K\varepsilon_0 tl}{d_{x2}},\ C_{x2} = n\frac{K\varepsilon_0 tl}{d_{x3}} + n\frac{K\varepsilon_0 tl}{d_{x4}} \quad (1)$$

where K is the dielectric constant for air, ε_0 is the permittivity of free space, $t \times l$ is the overlapping area of comb fingers, and n is the number of comb finger pairs.

When a gripping force is transmitted to the x directional force sensor, movable comb set-2 in Fig. 3 moves away from stationary comb set-3 and closer to stationary comb set-1. The gaps between comb fingers become $d_{x1} = d_0 - x$, $d_{x2} = d_0' + x$, $d_{x3} = d_0 + x$

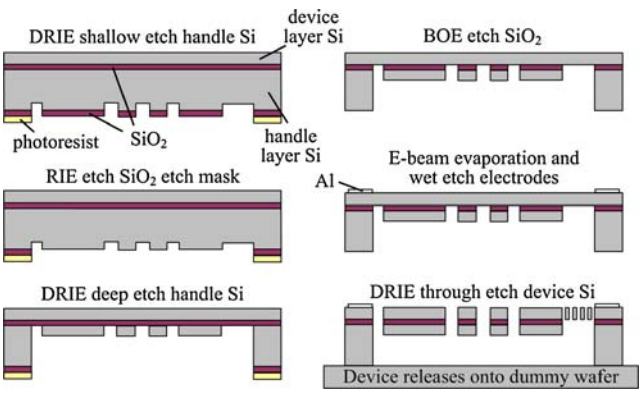

Fig. 2 Microfabrication process

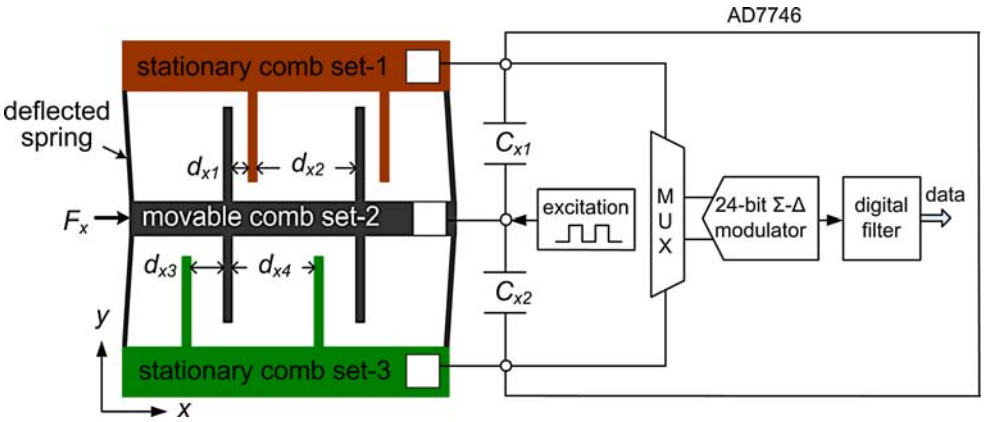

Fig. 3 Capacitive sensor schematic with a readout chip

and $d_{x4} = d'_0 - x$. A readout chip (AD7746, Analog Devices) read capacitance changes, and an interface program simultaneously calculated them into voltages according to

$$V_{out-x} = V_{ref}\left(\frac{C_{x1} - C_{x2}}{C_{x1} + C_{x2}}\right) = V_{ref}\frac{xd'_0 - xd_0}{d_0 d'_0 - x^2} \cong V_{ref}\frac{x}{d_0} \tag{2}$$

By initially setting $d_0 << d'_0$, the resulting output signal V_{out-x} can be proportional to the middle plate displacement x. Therefore, the undesired additional parallel capacitance effect can be minimized by placing repeated comb plate units reasonably far apart (e.g., $d_0 = 5$ μm and $d'_0 = 20$ μm in this design), and a high linearity was obtained (e.g., when $x < 2$ μm, linearity is better than 1.5%). The above analysis is also applicable to the y direction. Integrated two-axis capacitive force sensors were orthogonally configured. Structural-electrostatic coupled finite element simulation was conducted to determine spring dimensions and the placement of comb drives to maximize sensitivity while minimizing cross-axis coupling and nonlinearity.

Force sensor calibration was conducted using a precision microbalance (XS105DU, Mettler Toledo) with a resolution of 0.1 μN. Figure 4 shows the force sensor calibration results, demonstrating a high input-output linearity and minimized cross-axis coupling. The integrated force sensors are capable of resolving gripping forces up to 30 μN (resolution: 19.9 nN) and contact forces up to 58 μN (resolution: 38.5 nN).

The device employs a V-beam electrothermal microactuator connected to the lower part of a long gripping arm to generate large gripping displacements at gripping arm tips at low driving voltages. The temperature of the active gripping arm tip was measured using a fine-gauge thermocouple (CHCO-0005, Omega) with a 33 μm junction in diameter. The gripping arm tip moves by 32 μm at 6V; and due to the many heat-sink beams, the temperature at the gripping arm tip is

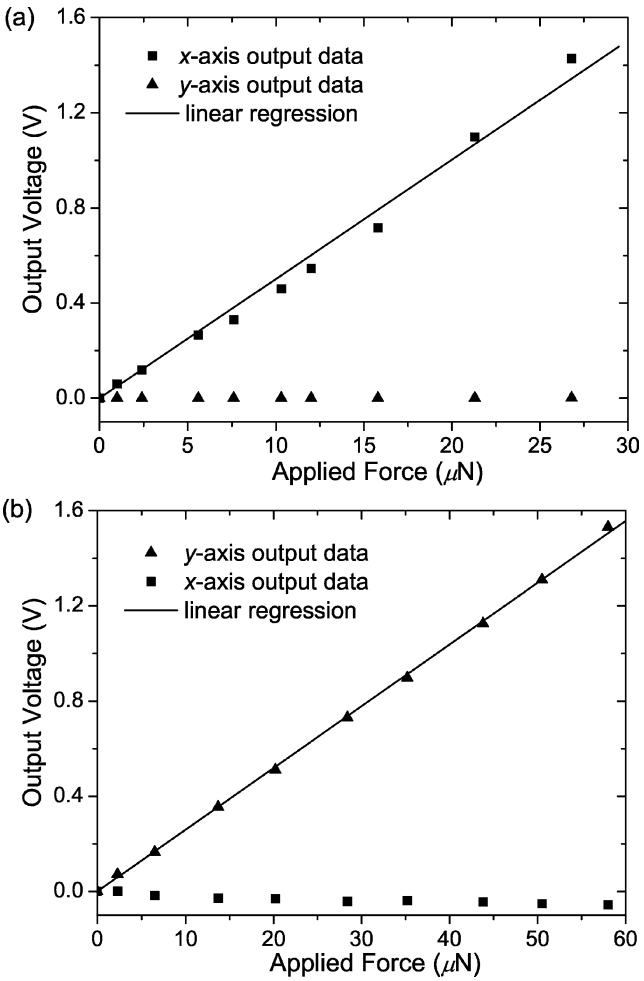

Fig. 4 Force sensor calibration results. Forces applied only (**a**) along the x direction; (**b**) only along the y direction. Also shown are coupled responses

29°C in air, demonstrating a low temperature suitable for biomaterial manipulation.

3 Materials and experimental methods

3.1 Preparation of microcapsules

Alginate sodium salt of medium molecular weight (viscosity of 2.0% solution 3,500 cps at 25°C) was purchased from Sigma (St. Louis, MO, USA). Ultrafine calcium carbonate powder (Miltifex-MM, 0.074 μm) was kindly donated by Special Minerals Inc. (Adams, MA, USA). Chitosan was purchased from Fluka (Buchs, SG, Switzerland) and modified before use by a free radical degradation method. Distilled and deionized (DDI) water was prepared by a Millipore (Billerica, MA, USA) system. A previous method (Liu et al. 2007) was modified to prepare alginate-chitosan microcapsules 20 μm in mean diameter. In brief, calcium carbonate powder was dispersed in an alginate solution, emulsified in light mineral oil containing Span 80 under stirring. Gelation of the particles was initiated by addition of acetic acid. The resultant microcapsules were recovered by centrifugation. The adsorption experiments were carried out for 30 min at 4°C, followed by incubation of the microcapsules in chitosan solutions of different concentrations (1%, 2%, 3%, w/v) in 0.3% (v/v) acetic acid for 10 min.

3.2 System setup

Figure 5 shows the experimental system setup. The system includes a 3-DOF microrobot (MP-285, Sutter) for positioning the microgripper, an inverted microscope (IX81, Olympus) with a CMOS camera (A601f, Basler), a microgripper wire-bonded to a custom designed readout circuit which was built around an ASIC (AD7746, Analog Devices) for measuring capacitance changes, and a motion control board (6259, National Instruments) mounted on a host computer.

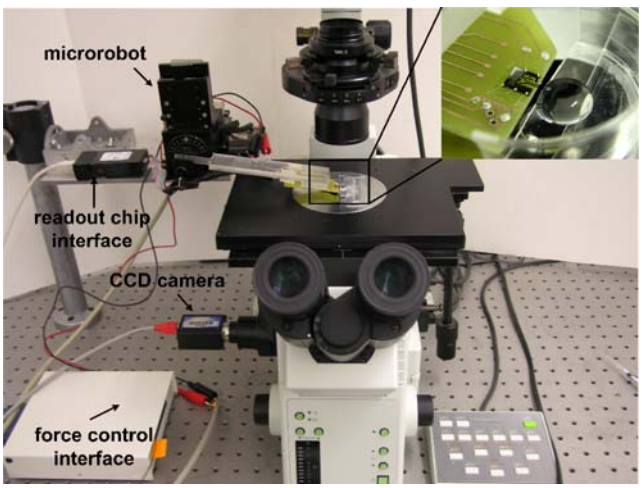

Fig. 5 Micromanipulation system. *Inlet picture* shows a wire-bonded microgripper with gripping arms immersed into a liquid droplet

3.3 Manipulation and micro-scale compression testing

A droplet of pH 7.4 Phosphate-Buffered Saline (PBS), which mimics *in vivo* environment, containing suspended alginate-chitosan microcapsules (ranging from 15–25 μm) was dispensed through pipetting on a petri dish. The microrobot controlled the microgripper to immerse the gripping arms into the liquid droplet and conducts manipulation and compression testing. The microgripper with a tilting angle of 10° was controlled by the microrobot to immerse the gripping arm tips into the PBS droplet while the microactuator and force sensors stayed outside.

The system conducted contact detection automatically based on the contact force feedback (Kim et al. 2008). The gripping arms then approached a microcapsule for grasping. Figure 6(a) illustrates the experimental situation where a microcapsule is held between gripping arms. Figure 6(b–d) is a series of snapshot pictures from the experiments showing the gripping arm tips continuously compressed a microcapsule inside PBS.

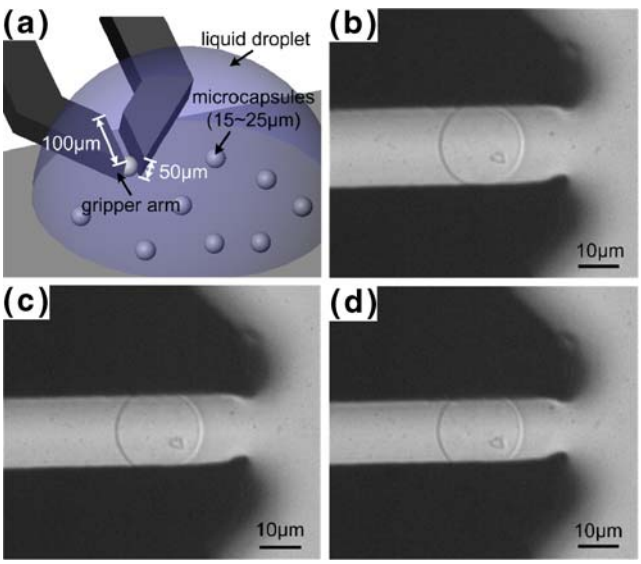

Fig. 6 (**a**) An illustration of experimental situation. (**b**) (**c**) (**d**)A series of snapshots for a microcapsule with 2% chitosan coating in PBS: (**b**) Start to compress the microcapsule; (**c**) 10% deformation at 374.65 nN; (**d**) 20% deformation at 962.28 nN

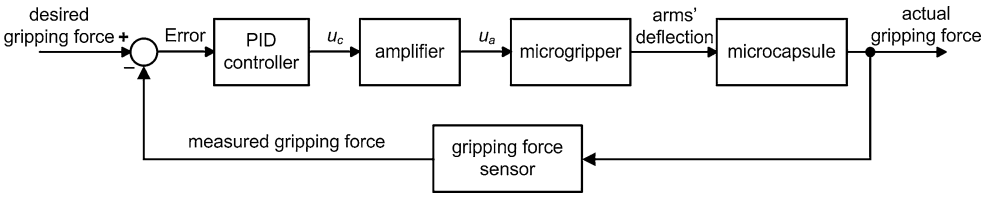

Fig. 7 Block diagram of force-controlled micrograsping

Gripping force data and image data were synchronously acquired by a custom built data acquisition program at a sampling frequency of 15 Hz. For elastic measurement, the gripping arm tips acting as two compressing plates increased gripping forces to continuously compress the microcapsule up to 20% deformation at a speed of 0.25 μm/s. For viscoelastic measurement, the active gripping arm was controlled at a speed of 5 μm/s to compress a microcapsule within 20% deformations and then held it in place to allow the microcapsule to creep with a constant force applied via a proportional-integral-derivative (PID) closed-loop force controller (Fig. 7).

Phase contrast images of deformed microcapsules were measured in real time during micrograsping using a visual tracking algorithm (Liu et al. 2007). Displacements of the gripping arm and the force sensing arm were tracked with a resolution of 0.08 pixel, from which deformations of the microcapsule were calculated. With the optical setup (40× objective, 0.6 NA, 0.26×0.26 μm pixel size), the measurement resolution of microcapsule deformations was determined to be 20.5 nm.

4 Results and discussion

4.1 Elastic property characterization

Force-displacement curves were collected simultaneously via force sensing signal and corresponding microscopic image data on 5 microcapsules of each type (1%, 2% and 3% chitosan coating). In order to quantify Young's modulus values, the force-displacement data need to be assessed by an appropriate mechanics model.

The Hertzian half-space contact mechanics model is widely used to characterize solid-like microparticles and biological cells.

$$\delta = \left[\frac{3(1-\nu^2)}{4E\sqrt{R}}\right]^{2/3} F^{2/3} \tag{3}$$

where δ and F are the compressive displacement and force, E is Young's modulus, R is the radius of a solid sphere, and ν is Poisson's ratio which is assumed to be 0.5 for incompressible materials.

Since the Hertzian model is only applicable to small deformations ($\delta/R < 0.1$) (Liu 2006), an extended mechanics model accommodating large deformations (Tatara 1993) was used in this work to assess experimental data. As shown in Fig. 8(a), the extensive relationship between displacement and force

$$\delta = \frac{3(1-\nu^2)F}{4Ea} - \frac{f(a)F}{\pi E} \tag{4}$$

$$f(a) = \frac{2(1+\nu)R^2}{(a^2+4R^2)^{3/2}} + \frac{1-\nu^2}{(a^2+4R^2)^{1/2}} \tag{5}$$

where a is the radius of contact area. The second term of Eq. 4 is due to the reaction force, $-F$, and can be neglected within small deformation range ($\delta/R < 0.1$). Thus, Eq. 3 can be derived from the generalized result of Eq. 4.

It was found that the value of compressive displacement δ calculated from Eq. 4 agrees better than the value calculated from Eq. 3 with the experimental data for a rubber sphere in the range $\delta/R < 0.2$. Above this range, the values of δ become much larger than experimental results mainly due to nonlinear elasticity of rubber (Tatara 1993). Therefore, we chose 20% deformation ($\delta/R < 0.2$) including an extensive term from the reaction force to assess global mechanical properties of the microcapsules and minimize the nonlinear effect, such as volume changes due to the drainage of liquid medium during compression.

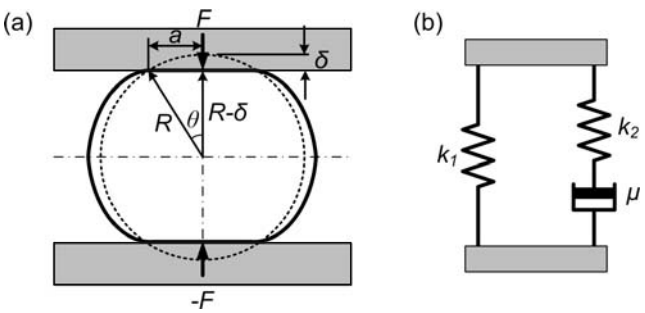

Fig. 8 Schematics for mechanics models. (**a**) Large elastic deformation model. (**b**) Kelvin model for determining viscoelastic parameters

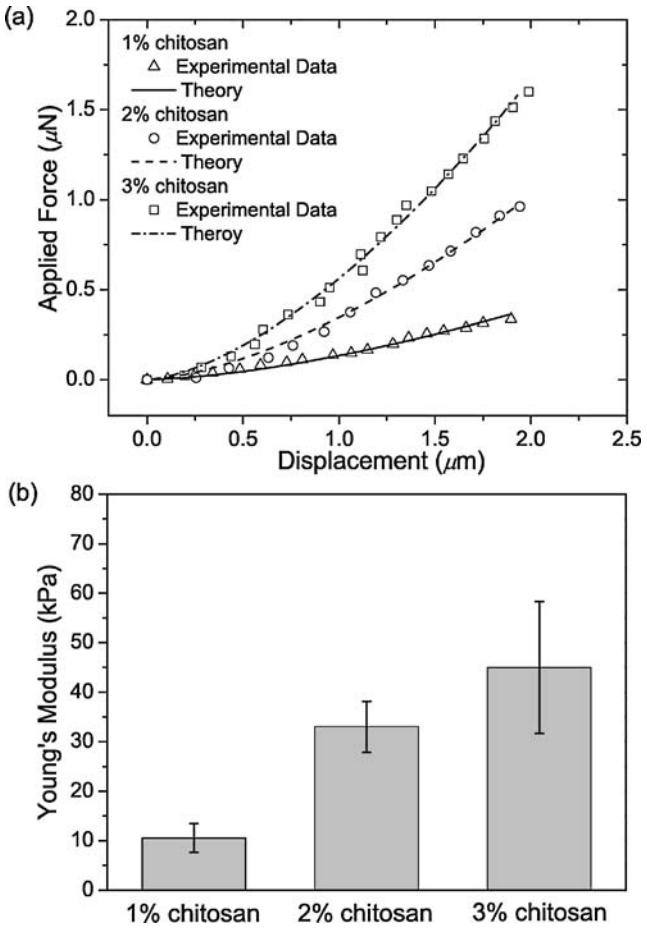

Fig. 9 Elastic characterization results. (**a**) Force-displacement curves collected on a microcapsule with 1%, 2%, and 3% chitosan coating and nonlinear curve fitting curves with Eq. 4 and (**b**) Young's modulus values of the microcapsules. *Error bars* represent means ± S.D. ($n = 5$)

Assuming that the lateral extension is not significant within 20% deformation, as shown Fig. 8(a), the radius of contact area ($0 < a < R$) as a function of compressive displacement δ can be geometrically calculated as

$$a = (R - \delta)\tan\theta \quad \text{and} \quad \theta = \cos^{-1}[(R - \delta)/R] \tag{6}$$

It was verified that the contact area obtained from Eq. 6 and measured from experimental images within 20% deformation were in agreement (differences < 5%)

Figure 9(a) shows representative force-displacement curves and nonlinear Levenberg-Marquardt curve fitting according to Eq. 4 for a microcpasule with 1%, 2% and 3% chitosan coating, respectively. Through curve fitting, Young's modulus values shown in Fig. 9(b) were determined to be 10.56 ± 2.94 kPa, 33.01 ± 5.13 kPa, and 44.99 ± 13.33 kPa for 1%, 2%, and 3% chitosan-coated microcapsules, respectively, which are comparable to Young's modulus of human erythrocytes (red blood cells), 26 ± 7 kPa (Dulinska et al. 2006).

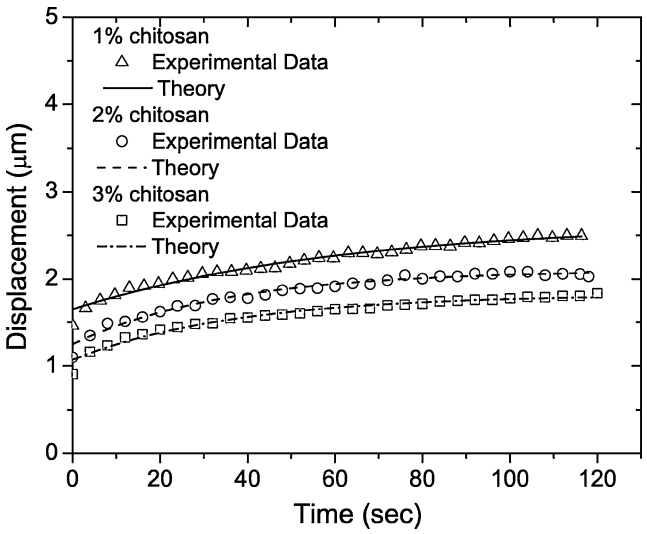

Fig. 10 Time-dependent displacement curves collected on a microcapsule with 1%, 2%, and 3% chitosan coating at 300 nN, 600 nN, and 800 nN, respectively and nonlinear curve fitting curves with Eq. 7

Although the shape of red blood cells (RBCs) is a parachute-like biconcave so that the deformation behavior would be different, the comparable modulus values indicate that the microcapsules at the physiological pH (i.e., pH 7.4) are as soft/deformable as RBCs and thus, may be mechanically suitable for intravenous injection use if they are made with the size of RBCs (e.g., 4–10 μm in diameter).

4.2 Viscoelastic property characterization

The "viscoelastic correspondence principle" states that if a solution to a linear elasticity problem is known, the solution to the corresponding problem for a linearly viscoelastic material can be obtained by replacing each quantity that is time dependent (Lakes 1998). Thus, applying the correspondence principle to Eq. 4 and employing the Kelvin model (Fig. 8(b)), the following viscoelastic model was derived to assess viscoelastic data in this work.

$$\delta(t) = \frac{2F_0}{3k_1}\left[\frac{3(1-\nu^2)}{4a_0} - \frac{f(a_0)}{\pi}\right]\left[1 + \left(\frac{\tau_\varepsilon}{\tau_\sigma} - 1\right)e^{-t/\tau_\sigma}\right] \tag{7}$$

Table 1 Viscoelastic parameters (Kelvin model) of microcapsules in pH 7.4 PBS

Chitosan%	k_1(kPa)	k_2(kPa)	μ(kPa·s)
1	6.70 ± 2.30	4.19 ± 1.25	133.48 ± 18.18
2	21.27 ± 5.77	13.60 ± 3.09	289.39 ± 73.89
3	29.13 ± 6.40	21.89 ± 6.87	562.09 ± 171.60

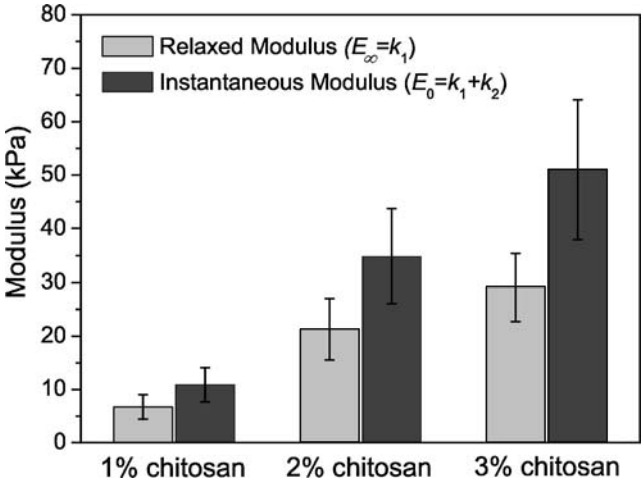

Fig. 11 Modulus values of 1%, 2% and 3% chitosan coated microcapsules obtained through viscoelastic characterization. *Error bars* represent means ± S.D. ($n = 5$)

where F_0 and a_0 are the instantaneous force and the radius of contact area, respectively, $\nu = 0.5$ is the Poisson's ratio for incompressible materials, k_1 is the relaxed modulus which is equal to E_∞, τ_ε is the force relaxation time constant, and τ_σ is the creep time constant. The instantaneous modulus is defined as $E_0 = k_1 + k_2$ and viscosity as $\mu = (\tau_\sigma - \tau_\varepsilon)k_1$ (Sato et al. 1990).

Figure 10 shows time-dependent displacements of a microcapsule under a constant force. Viscoelastic parameters were determined and summarized in Table 1. It can be seen that an increase in cross-linking percentage of chitosan results in a decrease in the relaxation rate of microcapsules. Comparing the experimental results of elastic and viscoelastic characterization, the relaxed modulus is related to Young's modulus shown in Fig. 9(b) by $E = 3E_\infty/2$, which is consistent with previous theoretical analysis (Sato et al. 1990), proving the validity of Eq. 7 for viscoelastic data assessment. Figure 11 summarizes modulus values obtained through viscoelastic characterization. The elastic and viscoelastic characterization results quantitatively reveal how chitosan cross-linking percentages affect the mechanical properties of the alginate-chitosan microcapsules.

5 Conclusion

This paper presented micro-scale compression testing of soft hydrogel microcapsules at wet state. The new technique is based on a monolithic MEMS microgripper with two-axis nanonewton force sensors. The microgripper manipulated highly deformable microcapsules in pH 7.4 PBS and simultaneously obtained force and displacement data for mechanical characterization. The compressive forces were obtained from gripping force feedback (force resolution: 19.9 nN), and material deformations were measured from phase contrast images (displacement measurement resolution: 20.5 nm). Force-displacement and time-dependent displacements data were collected on 1%, 2%, and 3% chitoan-coated alginate microcapsules (a total of 15 microcapsules that are 15–25 μm in diameter). Mechanics models were used to assess experimental data and quantify Young's modulus values and viscoelastic parameters of the microcapsules. The force-feedback microgripper enables an easy-to-operate technique for accurate compression testing of micrometer-sized biomaterials.

Acknowledgements This work was supported by the Natural Sciences and Engineering Research Council of Canada and by the Ontario Ministry of Research and Innovation.

References

A. Fontes, H.P. Fernandes, A.A. de Thomaz, L.C. Barbosa, M.L. Barjas-Castro, C.L. Cesar, J. Biomed. Opt. **13**, 014001 (2008)
R.M. Hochmuth, J. Biomech. **33**, 15 (2000)
I. Dulinska, M. Targosz, W. Strojny, M. Lekka, P. Czuba, W. Balwierz, M. Szymonski, J. Biochem. Biophys. Methods **66**, 1 (2006)
A.R. Bausch, W. Moller, E. Sackmann, Biophys. J. **76**, 573 (1999)
J. Blewett, K. Burrows, C. Thomas, Biotechnol. Lett. **22**, 1877 (2000)
V.V. Lulevich, O.I. Vinogradova, Langmuir **20**, 2874 (2004)
G. Lin, R.E. Palmer, K.S.J. Pister, K.P. Roos, IEEE Trans. Biomed. Eng. **48**, 996 (2001)
S. Yang, T. Saif, Rev. Sci. Instrum. **76**, 044301 (2005)
Y. Sun, S.N. Fry, D.P. Potasek, D.J. Bell, B.J. Nelson, J. Microelectromech. Syst. **14**, 4 (2005)
Y. Sun, K.T. Wan, K.P. Roberts, J.C. Bischof, B.J. Nelson, IEEE T. Nanobiosci. **2**, 279 (2003)
F. Beyeler, A. Neild, S. Oberti, D.J. Bell, Y. Sun, J. Dual, B.J. Nelson, J. Microelectromech. Syst. **16**, 7 (2007)
C. Yamahata, D. Collard, T. Takekawa, M. Kumemura, G. Hashiguchi, H. Fujita, Biophys. J. **94**, 63 (2008)
Q. Liu, A.M. Rauth, X.Y. Wu, Int. J. Pharm. **339**, 148 (2007)
K. Kim, X.Y. Liu, Y. Zhang, Y. Sun, J. Micromech. Microeng **18**, 055013 (2008)
X.Y. Liu, J.H. Tong, Y. Sun, Smart Mater. Struct. **16**, 1742 (2007)
K.K. Liu, J. Phys. D: Appl. Phys. **39**, R189 (2006)
Y. Tatara, J. Soc. Mech. Eng. Ser. A **36**, 190 (1993)
R. S. Lakes, *Viscoelastic Solids* (CRC, Boca Raton, 1998)
M. Sato, D.P. Theret, L.T. Wheelerand, N. Ohshima, R.M. Nerem, J. Biomech. Eng. **112**, 263 (1990)